

Theoretical structural phase stability of BeO to 1 TPa

J. C. Boettger and J. M. Wills

Theoretical Division, Los Alamos National Laboratory, Los Alamos, New Mexico 87545

(Received 15 December 1995; revised manuscript received 6 June 1996)

The equation of state and structural phase stability of BeO have been calculated for pressures up to 1 TPa using two all-electron, full-potential electronic-structure techniques; one using a linear muffin-tin orbital basis and the other a linear combination of Gaussian type orbitals basis. Both methods predict an as yet unobserved series of phase transitions, wurtzite→zinc blende→rocksalt, with the final transition at about 95 GPa. This nearly exact local-density approximation result disagrees with all earlier, more approximate, calculations by at least 40%. A theoretical Hugoniot, consistent with shock wave data up to 100 GPa, has been generated for BeO using electronic-structure results. [S0163-1829(96)03038-X]

It is well known that the structural phase stabilities of the $A^N B^{8-N}$ compounds can be related to their ambient spectroscopic ionicities (f_i) via the dielectric theory of Phillips and Van Vechten.^{1,2} According to this theory, binary compounds with $f_i > 0.785$ crystallize in a sixfold coordinated structure such as rocksalt (RS), while those with $f_i < 0.785$ crystallize in a fourfold structure such as zinc blende (ZB) or wurtzite (W).¹ Under pressure, the tetrahedral compounds with $f_i > 0.35$ first transform to an ionic sixfold structure and then to some metallic phase, while those with $f_i < 0.35$ transform to the metallic phase directly.^{1,2} Given this understanding, it is surprising that the pressure induced phase sequence for BeO is not yet fully understood.

BeO has a Phillips ionicity¹ of 0.602 and crystallizes in the W structure under ambient conditions, in accord with the dielectric theory. Since this f_i is similar to those of the Zn based IIB-VIA semiconductors, it is reasonable to expect BeO to undergo a fourfold to sixfold transition at a comparable pressure; i.e., roughly 9.5→18.0 GPa.² This expectation was supported by two early calculations.^{3,4} In the first, Chang and Cohen³ used the *ab initio* pseudopotential (AP) method to predict a W→RS transition at 22 GPa. In the second, Jephcoat *et al.*⁴ found the same transition at 40 GPa using the more approximate potential-induced-breathing (PIB) method. Neither of these predictions however is consistent with existing high pressure data. Raman spectra show no evidence of a phase transition in BeO for hydrostatic pressures up to 55 GPa,⁴ while Hugoniot data do not reveal any large volume change transitions for stresses up to 100 GPa.⁴ Jephcoat *et al.*⁴ noted that their 40 GPa prediction is not irreconcilable with the Raman data, since the W phase could remain metastable beyond the equilibrium boundary. It is difficult however to imagine that the W phase could persist for shock stresses up to 100 GPa if that boundary were at 40 GPa.

A more recent investigation⁶ of the phase stability of BeO using soft nonlocal pseudopotentials (SNP) predicted that the fourfold to sixfold transition should occur at 139 GPa. Although this result is consistent with the data,^{4,5} it also introduces a new problem. There now exist two local density approximation (LDA) pseudopotential predictions for the transition pressure that differ by more than a factor of 6. At least one of these results must be wrong. Thus it is not clear

what the exact LDA transition pressure is for BeO or how well that pressure agrees with the data.

To resolve these issues, we have calculated the stabilities of the W, ZB, and RS phases of BeO for pressures up to 1 TPa using two all-electron, full-potential electronic structure techniques; the full-potential linear muffin-tin orbital (FPLMTO) method⁷ and the linear combination of Gaussian type orbitals-fitting function (LCGTO-FF) method.⁸ Although both techniques include the contributions of all electrons explicitly, without the use of pseudopotentials, and do not impose any particular shape on the density or potential, they differ in nearly every other respect, thereby ensuring that their results are independent. Possible LDA sensitivity is accounted for by using different parametrizations of the exchange-correlation (XC) potential and energy density.^{9,10}

The FPLMTO method uses a basis of muffin-tin orbitals. Basis functions (scalar relativistic), electron densities, and potentials (using the Perdew-Zunger⁹ LDA) are expanded in spherical waves with numerical radial functions within non-overlapping site-centered spheres and in Fourier series in the interstitial region between the spheres. All spherical harmonic expansions extended through $l=8$. The Fourier expansions used roughly 350 plane waves per atom for basis functions and 3000 plane waves per atom for densities and potentials. The muffin-tin radii were chosen to bracket the minima in the density between atoms for all of the structures. After prescribing muffin-tin volumes for a particular unit cell volume, the muffin tins were maintained at a fixed fraction of the unit cell. This procedure provides comparable convergence of the Fourier series for all volumes and, judging by minimizing total energies, gives the most accurate results. The FPLMTO method allows inclusion of bases derived from different principal atomic quantum numbers but the same orbital quantum numbers in a single fully hybridizing basis set. The LMTO basis set is enriched by including multiple bases differing only in the interstitial kinetic energies. The current bases consisted of $3(2s,2p)$ and $2(3d)$ orbitals on O and $2(2s)$ and $3(3s,2p)$ orbitals on Be; where the premultiplicity gives the number of kinetic energies used. The Brillouin zone (BZ) integrals were done via Fourier quadrature¹¹ using 17 irreducible points for the W structure and 28 irreducible points for the RS and ZB structures.

The current implementation of the LGCTO-FF technique in the program GTOFF has been described in detail elsewhere.¹² The LCGTO-FF method is distinguished from other electronic structure methods by its use of three independent GTO basis sets to expand the orbitals, density, and XC integral kernels; here using the LDA parametrization of Hedin and Lundqvist.¹⁰ The orbital basis sets used here were an $8s4p$ primitive basis contracted to a $5s3p$ basis for the Be atoms and a $12s7p1d$ primitive basis contracted to an $8s4p1d$ basis for the O atoms. The charge/XC basis sets only included s -type GTO's, $7s/5s$ for Be and $8s/5s$ for O, because of the high degree of symmetry exhibited by the various structures. For the smaller volumes, the basis sets were modified slightly to avoid near linear dependencies. These basis sets can be obtained from the authors. BZ integrals were carried out with the histogram technique on a uniformly distributed mesh of k points including 17 irreducible points for the W structure and 16 irreducible points for the RS and ZB structures.

The FPLMTO method was used to calculate the total energy of BeO in the W , ZB, and RS structures at 9, 10, and 7 molecular volumes, respectively, ranging from 102 bohr³ down to 56 bohr³. Those energies were fitted with a third order polynomial in the hydrostatic Eulerian component¹³ $e = \frac{1}{2}[1 - (V_0/V)^{2/3}]$, where V_0 is the theoretical $P=0$ volume, to get the pressure, energy, and enthalpy as continuous functions of the volume. The fitted binding curves were then used to extract the properties of each phase at zero pressure and determine the structural phase sequence at high pressures.

In a similar fashion, the LCGTO-FF method was used to obtain total energies for the W and ZB structures at 8 molecular volumes ranging from 97.3 bohr³ down to 65.5 bohr³, while the total energy of the RS structure was calculated for 12 volumes ranging from 85.8 bohr³ down to 31.3 bohr³. The $P=0$ properties of the three structures were then obtained by fitting all of the W and ZB energies and eight of the RS energies with a modified universal equation of state (EOS).¹⁴ The calculated LCGTO-FF energies and fitted binding curves are shown in Fig. 1; the FPLMTO results do not differ significantly. To determine the phase sequence, the LCGTO-FF energies for the RS phase were refitted with two more volumes included.

Table I compares the FPLMTO and LCGTO-FF results for the equilibrium lattice constants (a_0), cohesive energies (E_c), and bulk moduli (B) with AP,³ PIB,⁴ and SNP (Ref. 6) results. Experimental data¹⁵ are given for the W structure. The two sets of all-electron, full-potential results are in good quantitative agreement, with the lattice constants, cohesive energies, and bulk moduli differing by no more than 0.3%, 0.4%, and 6%, respectively. This level of agreement suggests that the FPLMTO and LCGTO-FF methods both produce results that are reliable, reproducible representations of the LDA models being used. Thus the present results can be used to assess the precision of LDA results obtained with more approximate methods.

Comparison of the present results with the other theoretical results in Table I indicates that the pseudopotential results are reasonably good. The lattice constants produced with the SNP method⁶ are slightly smaller than the all-electron results. In contrast, the AP method³ yields lattice

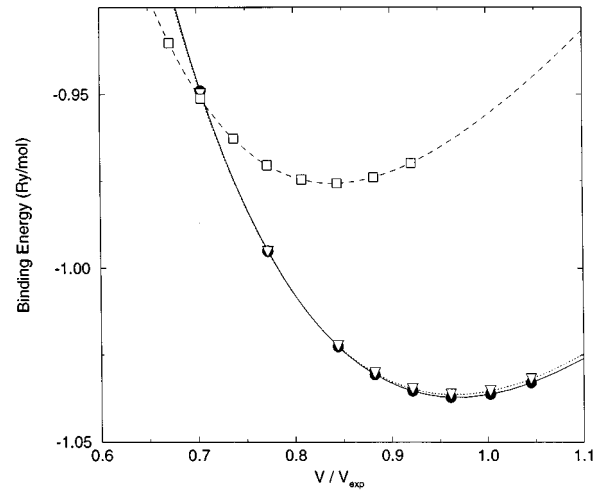


FIG. 1. LCGTO-FF binding energies (Ry) and fitted curves for the W (solid line and circles), ZB (dotted line and triangles), and RS (dashed line and squares) phases of BeO. ($V_{\text{expt.}}$ = experimental ambient volume; Ref. 15.)

constants that are in excellent agreement with the present results, but also produces bulk moduli that are significantly larger. The PIB method⁴ produces results that are notably different from those obtained with the various electronic-structure methods. In general, the present results for the W phase agree with experiment¹⁵ to the extent expected for state-of-the-art LDA electronic-structure calculations such as these. That is, the lattice constant exhibits the usual LDA-induced contraction relative to experiment and the bulk modulus is too large by 7→13%.

The sequence of pressure induced structural phase transitions was determined from crossings in the enthalpy ($H \equiv E + PV$) vs pressure curves for the various phases. For pressures up to 1 TPa, the FPLMTO and LCGTO-FF calcu-

TABLE I. Lattice constants (a_0 , bohr), cohesive energies (E_c , Ry/mol), and bulk moduli (B , GPa) for the various phases of BeO obtained with the FPLMTO, LCGTO-FF, SNP (Ref. 6), AP (Ref. 3), and PIB (Ref. 4) methods. Experimental data (Ref. 15) are listed for the W phase. Only the PIB calculations optimized c/a .

Phase	Method	a_0	c/a	E_c	B
W	FPLMTO	5.041	1.633	1.034	239
	LCGTO-FF	5.031	1.633	1.037	226
	SNP	4.987	1.629		228
	AP	5.034	1.623	1.06	283
	PIB	5.244	1.58		186
	Expt.	5.098	1.622		212
ZB	FPLMTO	7.121		1.033	229
	LCGTO-FF	7.108		1.036	240
	SNP	7.042			228
	AP	7.117		1.05	297
RS	FPLMTO	6.785		0.972	272
	LCGTO-FF	6.786		0.976	269
	SNP	6.748			266

TABLE II. Structural transition pressures (P_t , GPa), initial transition volumes (V_t ; bohr³/mol), and fractional volume changes ($\Delta V/V_t$) obtained for BeO with the FPLMTO, LCGTO-FF, SNP (Ref. 6), AP (Ref. 3), and PIB (Ref. 4) methods.

Trans.	Method	P_t	V_t	$\Delta V/V_t$
$W \rightarrow ZB$	FPLMTO	76.2	72.64	-0.002
	LCGTO-FF	62.8	74.71	-0.002
	SNP	74	70.70	-0.002
$ZB \rightarrow RS$	FPLMTO	94.1	70.04	-0.113
	LCGTO-FF	96.1	69.74	-0.112
	SNP	139	63.31	-0.099
$W \rightarrow RS$	FPLMTO	93.8	70.19	-0.114
	LCGTO-FF	95.4	69.98	-0.114
	SNP	137.3	63.95	-0.112
	AP	21.7	83.8	-0.202
	PIB	40	83.61	-0.108

lations both find the sequence to be $W \rightarrow ZB \rightarrow RS$. The transition pressures, initial transition volumes, and fractional volume changes obtained here are compared with other theoretical results in Table II.

For the $W \rightarrow ZB$ transition the FPLMTO, LCGTO-FF, and SNP methods produce transition pressures of 76, 63, and 74 GPa, respectively, all with the volume changes of only 0.2%. (Neither of the earlier investigations found a region of stability for the ZB structure.) Although the $W \rightarrow ZB$ transition pressures obtained here differ somewhat, the binding curves for those phases are so nearly parallel that the difference is not significant. Existing hydrostatic data⁴ cannot resolve between the predictions since both lie beyond the range of the data. Also, the structural energy difference between these phases is so small that the W phase would probably remain metastable beyond the equilibrium boundary in any low-temperature hydrostatic experiment. Moreover, the predicted volume change is too small to be detected in shock wave data.⁵ For these reasons, it is unlikely that the $W \rightarrow ZB$ transition will be observed in the near future.

For the higher pressure transition, $ZB \rightarrow RS$, the two all-electron, full-potential calculations are in nearly perfect agreement, again demonstrating the high precision achieved with both methods. The predicted transition pressure, about 95 GPa, lies well beyond the highest pressure attained in the hydrostatic experiments⁴ and is nearly coincident with the highest stress achieved in the shock experiments.⁵ Thus the current result is consistent with all existing data. The present results also indicate that the AP (Ref. 3) and PIB (Ref. 4) studies underestimated the “exact” LDA fourfold \rightarrow sixfold transition pressure by about 75% and 60%, respectively, while the SNP (Ref. 6) calculations overestimated that pressure by roughly 40%.

Since the highest pressure data available for BeO is the shock wave data,⁵ it is useful to derive a theoretical Hugoniot from the fitted 0 K isotherm. This has been done for the FPLMTO results using techniques that are employed routinely to generate global, tabular EOS's for the SESAME EOS library¹⁶ at Los Alamos National Laboratory. The

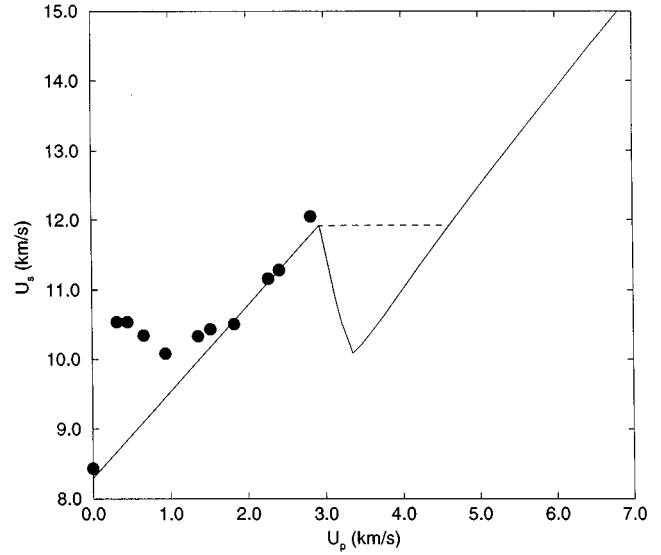


FIG. 2. Theoretical (line) and experimental (Ref. 5; circles) Hugoniot for BeO. (The dashed line indicates the predicted speed of the leading wave in the two-wave region.)

EOS's in the SESAME library are divided into three pieces: (1) a static lattice 0 K isotherm, (2) nuclear motion contributions at various temperatures, and (3) thermal electronic contributions for each temperature. This structure allows each component to be replaced without altering any other component. In this case, a global EOS for BeO was generated by replacing the static-lattice 0 K isotherm of an existing SESAME EOS for BeO (Ref. 17) with one derived from the FPLMTO calculations for the W and RS phases; i.e., without the ZB phase. The theoretical isotherm was adjusted to reproduce the experimental density¹⁵ by adding 2.17 GPa to each pressure and modifying the energies in a consistent fashion. The principal Hugoniot for BeO was then generated by applying the Rankine-Hugoniot jump conditions.¹⁸

The theoretical Hugoniot is shown in Fig. 2 in the form of a shock velocity (U_s) versus particle velocity (U_p) plot, along with experimental data.⁵ The calculated Hugoniot has two fundamental limitations. First, the theoretical curve is unphysical in the mixed-phase region since the true Hugoniot would exhibit a two-wave structure with the first wave having a constant shock velocity, indicated by the dashed line in Fig. 2. In addition, the experimental data include large strength effects that increase the measured shock velocity and stress relative to the theoretical Hugoniot. These effects will be most noticeable for small U_p and will diminish as U_p is increased. The one exception is the shock velocity at $U_p = 0$ (i.e., the sound velocity), which is measured ultrasonically.

Given these limitations, the overall agreement between theory and experiment is very good. The calculated Hugoniot provides a good match to the sound speed and the four larger U_p data points, for which the strength effects are smallest. As was noted earlier, the predicted transition pressure is nearly coincident with the highest measured shock stress. Thus the current result is fully consistent with the data and suggests that the experiment stopped just short of the transition. It also is obvious that the width of the mixed-phase

region is so large that it would be difficult to miss seeing the phase transition, if it occurred.

In summary, FPLMTO and LCGTO-FF calculations both predict that BeO undergoes a series of pressure induced phase transitions, $W \rightarrow ZB \rightarrow RS$, with the first transition at roughly 76 or 63 GPa and the second transition at about 95 GPa. Although there may be some question as to the existence and extent of the region of stability for the ZB phase, the current prediction for the final fourfold to sixfold transition is firm. This nearly exact LDA result disagrees with all

of the earlier, more approximate, calculations by at least 40%. The current predictions are consistent with existing experimental data.^{4,5} Thus it is clear that the fourfold to sixfold transition in BeO occurs at a pressure that is at least five times as large as the transition pressures of the other II-VI compounds with similar ionicities.

We thank P. E. Van Camp and V. E. Van Doren for providing a preprint of their results. This work was supported by the U.S. Department of Energy.

-
- ¹J. C. Phillips, *Bonds and Bands in Semiconductors* (Academic, New York, 1973); also see J. C. Phillips, *Rev. Mod. Phys.* **42**, 317 (1970).
- ²J. C. Phillips, *Phys. Rev. Lett.* **27**, 1197 (1971).
- ³K. J. Chang and M. L. Cohen, *Solid State Commun.* **50**, 487 (1984); also see K. J. Chang, S. Froyen, and M. L. Cohen, *J. Phys. C* **16**, 3475 (1983).
- ⁴A. P. Jephcoat, R. J. Hemley, H. K. Mao, R. E. Cohen, and M. J. Mehl, *Phys. Rev. B* **37**, 4727 (1988).
- ⁵S. P. Marsh, *High Pressures* **5**, 503 (1973); also see *LASL Shock Hugoniot Data*, edited by S. P. March (University of California, Berkeley, 1980), p. 241.
- ⁶P. E. Van Camp and V. E. Van Doren, *J. Phys. Condens. Matter* **8**, 3385 (1996).
- ⁷J. M. Wills and Olle Eriksson, *Phys. Rev. B* **45**, 13 879 (1992); J. M. Wills and B. R. Cooper, *ibid.* **42**, 4682 (1990); P. Söderlind, R. Ahuja, O. Eriksson, B. Johansson, and J. M. Wills, *Phys. Rev. B* **49**, 8365 (1994); M. Alouani, J. W. Wilkins, R. C. Albers, and J. M. Wills, *Phys. Rev. Lett.* **71**, 1415 (1993).
- ⁸J. C. Boettger, *Int. J. Quantum Chem. Symp.* **27**, 147 (1993); also see J. C. Boettger and S. B. Trickey, *Phys. Rev. B* **32**, 1356 (1985); J. W. Mintmire, J. R. Sabin, and S.B. Trickey, *ibid.* **26**, 1743 (1982).
- ⁹J. Perdew and A. Zunger, *Phys. Rev. B* **23**, 5048 (1981).
- ¹⁰L. Hedin and B. I. Lundqvist, *J. Phys. C* **4**, 2064 (1971).
- ¹¹S. Froyen, *Phys. Rev. B* **39**, 3168 (1989).
- ¹²J. C. Boettger, *J. Quantum Chem. Symp.* **29**, 197 (1995).
- ¹³F. Birch, *J. Geophys. Res.* **83**, 1257 (1978).
- ¹⁴A. Banerjea and J. R. Smith, *Phys. Rev. B* **37**, 6632 (1988); for the exact form used see, J. C. Boettger and S. B. Trickey, *ibid.* **53**, 3007 (1996).
- ¹⁵R. M. Hazen and L. W. Finger, *J. Appl. Phys.* **59**, 3728 (1986).
- ¹⁶S. Lyon and J. D. Johnson (unpublished).
- ¹⁷J. C. Boettger and J. M. Wills (unpublished).
- ¹⁸M. H. Rice, R. G. McQueen, and J. M. Walsh, *Solid State Phys.* **6**, 1 (1958).